Real-Time Integrity Monitoring for Civil Aviation with Improved Navigation Performance

Jin Chang · Xingqun Zhan* **· Yawei Zhai**

Shanghai Jiao Tong University

Abstract With the worldwide development in the past decades, multi-constellation of Global Navigation Satellite Systems (GNSS) are able to provide consistent and reliable navigation services today, which are expected to bring significant performance improvement to civil aviation in the future. For the GNSS based aircraft navigation, meeting the integrity and continuity requirements is of the most importance. In the currently proposed baseline Advanced Receiver Autonomous Integrity Monitoring (ARAIM) user algorithm, the integrity risk is evaluated using a conservative upper bound. Despite of its computational efficiency, this bound is not tight enough, which may lead to overly conservative results. Operationally, the system may incorrectly alert the user, which severely impacts navigation continuity. Therefore, in this work, we develop a new method to tightly bound the integrity risk, and establish a multi-constellation ARAIM test platform to validate the theory. The new approach takes advantage of the independence between position estimation error and detection test statistics, and expresses the integrity risk evaluation as a convex optimization problem. It is shown that the global maximum of the objective function is a tight bound on integrity risk, and it can be efficiently computed using an numerical method. Other than the theoretical derivations, another major contribution of this work is prototyping the ARAIM user segment in the Guidance, Navigation and Control (GNC) laboratory at Shanghai Jiao Tong University. Both of the ARAIM Multiple Hypothesis Solution Separation (MHSS) algorithm and the new approach are incorporated into the prototype, and the real-time integrity monitoring results are visually displayed in terms of horizontal and vertical protection levels, effective monitoring threshold, integrity risk, etc. As compared to the existing MHSS theory, the results suggest that the navigation service availability can be noticeably improved using the proposed method, especially when the constellations are subject to larger ranging errors.

1 Introduction

Nowadays navigation system is indispensable for civil air transportation. Navigation system allows aircraft to determine its location and to fly on a predetermined route. This can avoid many hazardous aviation accidents. For instance, when aircraft drifts off course, pilot is able to correct the error of position with navigation system. To build a robust navigation system, several work have been made in the past century. Before 1970s, the research of aircrafts navigation system focused on Radio Navigation System (RNS) and Inertial Navigation System (INS). But these two systems both have drawbacks such as limited system coverage and increasing navigation errors over time [1]. After 1970s, satellite-based positioning system which provides users with global coverage and lower positioning error began to flourish [2].

From the 1970s up to the present, many countries and regions have established their own satellite-based positioning systems such as Global Navigation System (GPS, U.S.A), GLONASS (Russia), BeiDou Navigation Satellite System (BDS, China), Galileo (Europe). At the same period, some augmentation systems, like Ground-Based Augmentation System (GBAS) and

* Corresponding Author: Xingqun Zhan,
E-mail: xqzhan@sjtu.edu.cn

Satellite Based Augmentation Systems (SBAS), have been built to improve the navigation performance. The combination of these satellite-based positioning systems (GPS, BDS, GLONASS, Galileo) is referred to as Global Navigation Satellite System (GNSS) and each individual satellite-based positioning system is termed as constellation [3].

For civil aviation, navigation system which meets stringent requirements is critical to guarantee the safety during the flight. The International Civil Aviation Organization (ICAO) put forward some metrics for satellite-based positioning system [4]. Two of the most challenging requirements for civil aviation are integrity and continuity [5]. Integrity is a measure of trust, which is used to determine whether the positioning solution provided by the navigation system is correct. Continuity measures navigation system's ability to operate without unplanned interruptions [4]. Receiver Autonomous Integrity Monitoring (RAIM) is a system that can provide users with real-time integrity monitoring results [6]. When satellite fault occurs during the flight, timely warning can be sent by RAIM to users. After mid-1990s, by using single frequency signal and single constellation, RAIM has become a backup navigation tool and it can be apply to en-route flight [5]. But previous research has found the drawbacks of RAIM. One of the major drawbacks is occasional lack of availability [7].

With the great development of satellite-based positioning system, single frequency signal and single constellation positioning is gradually replaced by dual frequency signal and multi-constellation positioning because it possesses two advantages. (a) Dual frequency signal can cancel the ionosphere delay [8]. (b) Multi-constellation positioning with increased number of satellites improves users geometry [9].

Due to these two advantages, dual frequency signal and multi-constellation positioning can significantly improve the accuracy and stability of positioning [10]. The superiority and greater redundancy of dual frequency multi-constellation positioning lead to consider making up the shortcomings of RAIM . So Advanced Receive Autonomous Monitoring (ARAIM) has been put forward to overcome these shortcomings. Many researchers have made great contributions to this. For instance, professor Juan Blanch from Stanford University and professor Boris Pervan from Illinois Institute of Technology have already built a solid theoretical foundation for ARAIM Multiple Hypothesis Solution Separation (MHSS) algorithm. Some institutions, take Stanford GPS Lab as an example, have devised ARAIM prototype that can be equipped on aircraft. Though dual frequency signal and multi-constellation position-

ing has better accuracy and greater redundancy for integrity monitoring, it also brings the higher probability of having faulted satellites which can severely affect the positioning solution.

Since the current augmentation systems, SBAS and GBAS, cannot cover every region of the world [11][12], it is urgent to develop ARAIM MHSS algorithm for the place with poor navigation performance. ARAIM MHSS algorithm enables aircraft to detect navigation fault and to correct positioning result by excluding some faulty satellites or constellations. Meanwhile, todays ARAIM MHSS algorithm also has some weaknesses, one of them is that the probability bound of ARAIM algorithm is not tight enough, which can significantly affect navigation performance especially when there exists exclusion function in ARAIM algorithm. To avoid this weakness, we propose a new approach of calculating the probability bound and establish multi-constellation ARAIM test platform to validate the theory.

The second part of this paper will introduce the basic principles of ARAIM. The third part of this paper focuses on introducing the new approach. In this chapter, the probability bound will be rewritten mathematically and new Probability of Hazardous Misleading Information (PHMI) equation will be introduced. The fourth part of this paper explains the working principles of multi-constellation ARAIM test platform. The fifth part of this paper shows the navigation performance under different condition(MHSS algorithm and new approach).

2 ARIAM Overview

2.1 ARAIM Background

Based on linearized pseudo-range equations, GNSS receiver can compute the users location by solving linear algebraic equation, which can be expressed as:

$$\mathbf{y} = \mathbf{H}\mathbf{x} + \boldsymbol{\epsilon} + \mathbf{f} \tag{1}$$

where $\mathbf{y}$ is a $n \times 1$ measurement vector, this vector represents the corrected pseudorange of satellites. $\mathbf{H}$ is a $n \times (3 + N)$ matrix in which n and N are the number of satellites and constellations, respectively. $\mathbf{x}$ is a $(3 + N) \times 1$ vector, which includes the users location and the clock error of different constellations. $\boldsymbol{\epsilon}$ is the noise, which comes from clock error, ephemeris error, tropospheric error, multipath, receiver noise and it follows normal distribution. $\mathbf{b}$ and $\mathbf{V}$ are defined as bias vector and covariance matrix of $\boldsymbol{\epsilon}$ respectively. $\mathbf{f}$

is a $n \times 1$ vector, which indicates the fault magnitude of navigation system. The solution of equation Eq.(1) is all-in-view estimation positioning solution and it can be written as:

$$\hat{\mathbf{x}}_0 = (\mathbf{H}^T\mathbf{V}^{-1}\mathbf{H})^{-1}\mathbf{H}^T\mathbf{V}^{-1}\mathbf{y} \qquad (2)$$

When one satellite or more satellites that corresponds to the i th fault model was excluded, satellite-removed positioning solution $\hat{\mathbf{x}}_i$ can be written as:

$$\hat{\mathbf{x}}_i = (\mathbf{H}^T\mathbf{V}_i^{-1}\mathbf{H})^{-1}\mathbf{H}^T\mathbf{V}_i^{-1}\mathbf{y} \qquad (3)$$

$\mathbf{V}_i$ in Eq.(3) is the covariance matrix which excludes the faulty satellite or satellites corresponding to i th fault model. For i th fault model, we assume that p th satellite is in i th fault model and q th satellite is faultless. Based on this assumption, we can compute covariance matrix $\mathbf{V}_i$ below:

$$\mathbf{V}_i(p,p) = 0, \quad \mathbf{V}_i(q,q) = \mathbf{V}(g,g) \qquad (4)$$

$$\hat{\mathbf{x}}_{ex,k} = (\mathbf{H}^T\mathbf{V}_{ex,k}^{-1}\mathbf{H})^{-1}\mathbf{H}^T\mathbf{V}_{ex,k}^{-1}\mathbf{y} \qquad (5)$$

When considering MHSS ARAIM exclusion function, we introduce $\mathbf{V}_{ex,k}$, which excludes the k th subset fault model, under the ex th fault model. For fault model ex and the subset fault model k, we assume that the p th satellite is in the ex th fault model or the k th subset fault model and q th satellite is faultless. Based on this assumption, we can compute covariance matrix $\mathbf{V}_{ex,k}$ bellow:

$$\mathbf{V}_{ex,k}(p,p) = 0, \quad \mathbf{V}_{ex,k}(q,q) = \mathbf{V}(q,q) \qquad (6)$$

If fault model ex and subset fault mode k have been excluded, the estimation positioning solution can be written as:

$$\hat{\mathbf{x}}_{ex,k} = (\mathbf{H}^T\mathbf{V}_{ex,k}^{-1}\mathbf{H})^{-1}\mathbf{H}^T\mathbf{V}_{ex,k}^{-1}\mathbf{y} \qquad (7)$$

By using Eq.(1), Eq.(2), Eq.(4), error test statistic ϵ_0 and detection test statistic Δ_i can be defined as:

$$\epsilon_0 = \hat{\mathbf{x}}_0 - \mathbf{x}, \quad \epsilon_0 \sim (\mu_{HI,0}, \quad \mathbf{P}_0) \qquad (8)$$

where $\mu_{HI,0}$ and $\mathbf{P}_0$ are equal to $\mathbf{S}_0\mathbf{f} + \mathbf{S}_0\mathbf{b}$ and $(\mathbf{H}^T\mathbf{V}^{-1}\mathbf{H})^{-1}$ respectively.

$$\Delta_i = \hat{\mathbf{x}}_0 - \hat{\mathbf{x}}_i, \quad \Delta_i \sim (\mu_{HI,i}, \quad \mathbf{P}_i) \qquad (9)$$

where $\mu_{ND,i}$ and $\mathbf{P}_i$ are equal to $\mathbf{S}_0\mathbf{f} + \mathbf{S}_0\mathbf{b} - \mathbf{S}_i\mathbf{b}$ and $(\mathbf{H}^T\mathbf{V}_i^{-1}\mathbf{H})^{-1} - (\mathbf{H}^T\mathbf{V}^{-1}\mathbf{H})^{-1}$ respectively.

$\mathbf{S}_0$ and $\mathbf{S}_i$ are equal to $(\mathbf{H}^T\mathbf{V}^{-1}\mathbf{H})^{-1}\mathbf{H}^T\mathbf{V}^{-1}$ and $(\mathbf{H}^T\mathbf{V}_i^{-1}\mathbf{H})^{-1}\mathbf{H}^T\mathbf{V}_i^{-1}$ respectively.

By using Eq.(1), Eq.(3), Eq.(5), for the second layer detection of MHSS ARIAM, error test statistic ϵ_{ex} and detection test statistic $\Delta_{ex,k}$ can be defined as:

$$\epsilon_{ex} = \hat{\mathbf{x}}_{ex} - \mathbf{x}, \quad \epsilon_{ex} \sim (\mu_{HI,ex}, \quad \mathbf{P}_{ex}) \qquad (10)$$

where $\mu_{HI,ex}$ and $\mathbf{P}_{ex}$ are equal to $\mathbf{S}_{ex}\mathbf{b}$ and $(\mathbf{H}^T\mathbf{V}_{ex}^{-1}\mathbf{H})^{-1}$ respectively.

$$\Delta_{ex,k} = \hat{\mathbf{x}}_{ex,k} - \hat{\mathbf{x}}_{ex}, \quad \Delta_{ex,k} \sim (\mu_{ND,ex}, \quad \mathbf{P}_{ex,k}) \qquad (11)$$

where $\mu_{ND,ex}$ and $\mathbf{P}_{ex,k}$ are equal to $\mathbf{S}_{ex}\mathbf{b}$ and $(\mathbf{H}^T\mathbf{V}_{ex}^{-1}\mathbf{H})^{-1}$ respectively.

$\mathbf{S}_{ex,k}$ are equal to $(\mathbf{H}^T\mathbf{V}_{ex,k}^{-1}\mathbf{H})^{-1}\mathbf{H}^T\mathbf{V}_{ex,k}^{-1}$ respectively.

In the following paper, ARAIM is referred to as MHSS ARAIM.

2.2 ARAIM User Algorithm

ARAIM user algorithm consists of five functions:

(1) Analyzing the fault models

In practice, the number of fault models increases sharply with the number of satellites and constellations. To reduce computational burden, ARAIM user algorithm do not need to monitor all the fault models. Based on required threshold P_{thresh} (8×10^{-8}) [13][14][15], the sum of unmonitored fault models should meet the following requirement:

$$\sum_{j=1}^{h} P_j <= P_{thresh} \qquad (12)$$

where P_j is the probability of the j th unmonitored fault model occurring in navigation system and h is the number of unmonitored fault models.

(2) Determining detection and exclusion threshold

Detection threshold T_i can be derived from the allocated probability P_{FA_NE}, which represents the probability that test statistic Δ_i exceeds their threshold under fault-free hypothesis [13][14].

To calculate the exclusion threshold $T_{ex,k}$, we use the allocated probability P_{FD_NE}, which represents the probability that test statistic $\Delta_{ex,k}$ exceeds its threshold under second layer fault-free hypothesis [13][14].

(3) Evaluating ARAIM user algorithms availability

Before conducting the fault detection and exclusion function, the availability of ARAIM algorithm need to be evaluated. If ARAIM user algorithm is not available, the algorithm will skip the fault detection and exclusion functions. The requirement of ARAIM availability depends on different application scenarios. LPV-200 is a stringent requirement for ARAIM in approach phase. LPV-200 requirements of availability are: (a) Vertical Protection Level (VPL) is lesser than Vertical Alert Limit (VAL) (VPL $\leq$ 35 m) (b) Effective Monitor Threshold (EMT) $\leq$ 15 m. (c) 95% of the time, vertical accuracy $\leq$ 4 m. (d) 99.99999% of the time, fault-free vertical accuracy $\leq$ 10 m. The method of calculating VPL can derived from the equation of PHMI.

(4) Fault detection

When ARAIM algorithm is available, fault detection function can be conducted. The result of fault detection function depends on the equation below:

$$\Delta_{i,d} = |\mathbf{x}_{0,d} - \mathbf{x}_{k,d}| \qquad (d = 1, 2, 3) \tag{13}$$

where the subscript d represents the horizontal ($d = 1, 2$) and vertical ($d = 3$) direction. If $\Delta_{i,d}$ is larger than detection threshold $T_{i,d}$, it shows that the fault is detected by ARIAM user algorithm and fault exclusion function is about to exclude the fault. Otherwise, the algorithm skips the fault exclusion function.

(5) Fault exclusion

If fault has been detected, exclusion function attempts to correct the navigation solution by excluding some satellites or constellations. To determine the correctness of exclusion, we introduce $\Delta_{ex,k,d}$, which can be expressed by the following:

$$\Delta_{ex,k,d} = |\mathbf{x}_{ex,d} - \mathbf{x}_{ex,k,d}| \qquad (d = 1, 2, 3) \tag{14}$$

when $\Delta_{ex,k,d}$ is larger than exclusion threshold $T_{ex,k,d}$, it shows that the fault cannot be eliminated by ARAIM algorithm and the user needs to be alerted.

3 Optimized ARAIM Algorithm

3.1 Tighter Bound of PHMI

PHMI evaluation is of great importance in ARAIM user algorithm. This evaluation can monitor the efficiency of algorithm. But the current evaluation of PHMI accumulate errors in summation process. This may lead to safety problems.

To calculate PHMI more precisely, we use the independence of ϵ_0 and Δ_i, ϵ_{ex} and $\Delta_{ex,k}$ [17] to simplify the current PHMI equation. The simplified form can be given by:

$$P_{HMI} \leq P(|\epsilon_0| > l|H_0)P_{H0} +$$
$$\sum_{i=1}^{m} \max_{\mathbf{f}_i} \left(P(|\epsilon_0| > l|H_i, \mathbf{f}_i) \cdot P(|\Delta_i| < T_i|H_i, \mathbf{f}_i) \right) P_{H_i} +$$
$$\sum_{ex=1}^{m} (P(|\epsilon_{ex}| > l|H_0)P_{H_0} + P(|\epsilon_{ex}| > l|H_{ex})P_{H_{ex}} +$$
$$\sum_{\substack{k=1 \\ k \neq ex}}^{m_1} \max_{\mathbf{f}_k} \left(P(|\epsilon_{ex}| > l|H_k, \mathbf{f}_k) \cdot \right.$$
$$\left. P(|\Delta_{ex,k}| < T_{ex,k}|H_k, \mathbf{f}_k)) \right) P_{H_k} \tag{15}$$

where $\max\limits_{\mathbf{f}_i}$ and $\max\limits_{\mathbf{f}_k}$ represent the function of calculating the maximum value under fault model i and subset fault model k. $\mathbf{f}_i$ and $\mathbf{f}_k$ are the fault magnitude corresponding to the fault model i and subset fault model k. m and m_1 are the number of fault models that need to be monitored in detection function and exclusion function.

The first term of Eq.(15) is PHMI of detection function under fault free condition, so fault magnitude does not exist in this term.

For the second term of Eq.(15), it indicates a condition that the fault has existed in navigation system but detection function fail to detect the fault. We denote $P_{HI,i,d}$ and $P_{ND,i,d}$ as $P(|\epsilon_0| > l|H_i, \mathbf{f}_i)$ and $P(|\Delta_i| < T_i|H_i, \mathbf{f}_i)$ respectively. In Chapter 2, we explained the bias and variance of random variable ϵ_0 and Δ_i. These numerical characteristics can rewrite the second term of Eq.(15) mathematically.

As for $P_{HI,i,d}$, it can be rewritten as:

$$P_{HI,0,d} = 1 - \int_{-l_d}^{l_d} \frac{1}{\sqrt{2\pi \mathbf{P}_0(d,d)}} exp\left(\frac{(x - \mu_{HI,0,d})^2}{2\mathbf{P}_0(d,d)} \right) dx \tag{16}$$

where $\mathbf{P}_0$ is covariance matrix of ϵ_0 and $\mu_{HI,i,d}$ can be written as:

$$\mu_{HI,0,d} = \sum_{e=1}^{n} |\mathbf{S}_0(d,e)| \mathbf{b}(e,d) + \sum_{e=1}^{n} |\mathbf{S}_0(d,e)| \mathbf{f}_i(e,1) \tag{17}$$

For $P_{ND,i,d}$, it can be written as:

$$P_{ND,i,d} = \int_{-T_{\Delta_d}}^{T_{\Delta_d}} \frac{1}{\sqrt{2\pi \mathbf{P}_i(d,d)}} exp\left(\frac{(y - \mu_{ND,i,d})^2}{2\mathbf{P}_i(d,d)} \right) dy$$

$$(18)$$

where $\mathbf{P}_i$ is covariance matrix of Δ_i and $\mu_{ND,i,d}$ can be written as:

$$
\mu_{ND,i,d} = -\sum_{e=1}^{n} |\mathbf{S}_0(d,e) - \mathbf{S}_i(d,e)| \mathbf{b}(e,d)
$$
$$
+ \sum_{e=1}^{n} |\mathbf{S}_0(d,e)| \mathbf{f}_i(e,1)
$$

$$(19)$$

Since the only variable in equation Eq.(17) and Eq.(19) is $\mathbf{f}_i$, we can rewrite $P_{HI,i,d} \cdot P_{ND,i,d}$ as:

$$
P_{HMI,2} = P_{HI,i,d} \cdot P_{ND,i,d}
$$
$$
= k_i \int_{-T_{\Delta_d}}^{T_{\Delta_d}} \exp\left(\frac{(y - M + b_i)^2}{2\mathbf{P}_i(d,d)} \right) dy -
$$
$$
k_i k_0 \int_{-l_d}^{l_d} \int_{-T_{\Delta_d}}^{T_{\Delta_d}} \exp\left(-\frac{(y - M + b_i)^2}{2\mathbf{P}_i(d,d)} \right)
$$
$$
\exp\left(-\frac{(x - M - b_0)^2}{2\mathbf{P}_0(d,d)} \right) dx\,dy
$$

$$(20)$$

where $k_i = \frac{1}{\sqrt{2\pi\mathbf{P}_i(d,d)}}$, $k_0 = \frac{1}{\sqrt{2\pi\mathbf{P}_0(d,d)}}$, $y - M + b_i = y - \mu_{ND,i,d}$ and $x - M - b_0 = x - \mu_{HI,0,d}$. The subscript 2 in $P_{HMI,2}$ represents the second term of Eq.(15). Fig. 1 shows the image function of Eq.(15), Eq.(17) and Eq.(19).

In Eq.(16) and Eq.(18), b_0 and b_i are defined as positive and negative values, respectively. This definition takes into account the worst-case scenario. Under this definition, the maximum value of PHMI can be obtained. In Fig. 2 and Fig. 3 , we discuss four conditions of b_0 and b_i ($b_0 > 0, b_0 < 0, b_i > 0, b_i < 0$). Fig. 2 shows the function image of $P_{HI,0,d}$ and $P_{ND,0,d}$.
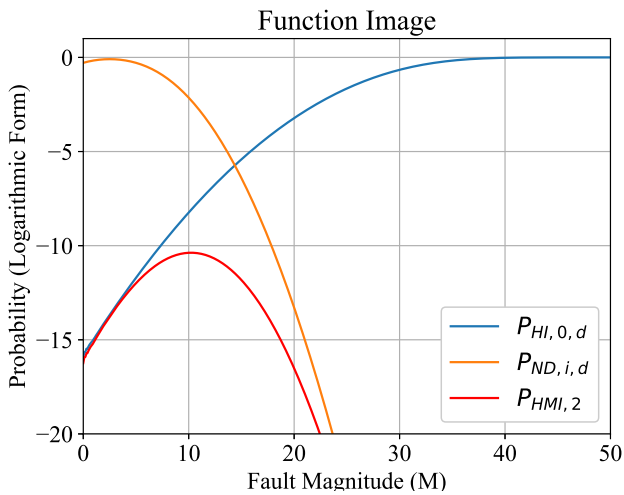
Fig. 1 Function Image (Logarithmic Form) of $P_{HI,0,d}$ $P_{ND,i,d}$ and $P_{HI,0,d} \cdot P_{ND,i,d}$
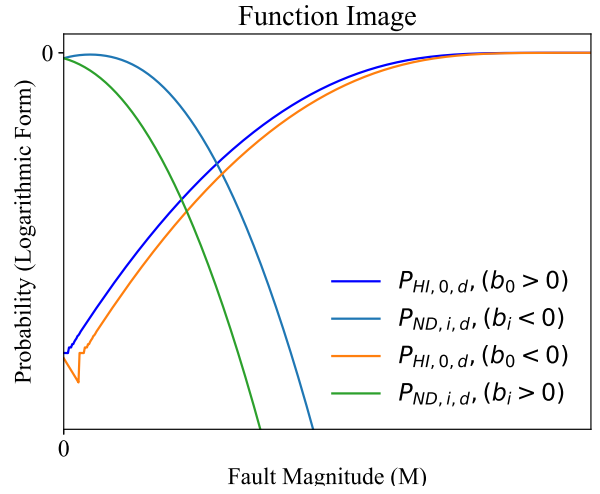
Fig. 2 Function Image (Logarithmic Form) of $P_{HI,0,d}$ and $P_{ND,i,d}$ with Different Biases
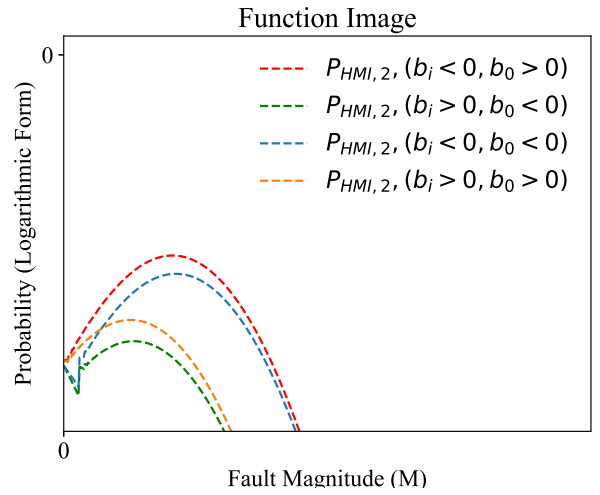
Fig. 3 Function Image (logarithmic form) of $P_{HI,0,d} \cdot P_{ND,i,d}$ with Different Biases

In Fig. 2 , the function images of $b_0 > 0$ and $b_i < 0$ are above the other function images so their product is lager than other conditions. Fig. 3 is the function image of $P_{HMI,2}$ under different conditions. It shows that the product of $P_{HI,0,d}(b_0 > 0)$ and $P_{ND,i,d}(b_i < 0)$ is above other function images. So we draw the conclusion that the product of $b_0 > 0$ and $b_i < 0$ can be used in calculating the maximum value of PHMI.

The third and the fourth term in Eq.(16) are the PHMI of exclusion function which are under fault free condition and right exclusion condition respectively. So fault magnitude does not exist in these two terms.

For the fifth term of Eq.(15), it indicates a condition that even exclusion function has excluded some satellites but the fault still exist in navigation system

and the second layer detection fail to detect the fault. We denote $P_{HI,ex,d}$ and $P_{ND,ex,d}$ as $P(|\epsilon_{ex}| > l|H_k, \mathbf{f}_k)$ and $P(|\Delta_{ex,k}| < T_{ex,k}|H_k, \mathbf{f}_k)$ respectively. In Chapter 2, we explained the bias and variance of random variable ϵ_{ex} and $\Delta_{ex,k}$. Similar to the derivation of formula Eq. (20), these numerical characteristics can rewrite the fifth term of Eq. (15) mathematically.

For $P_{HI,ex,d}$, it can be rewritten as:

$$P_{HI,ex,d} = 1 - \frac{1}{\sqrt{2\pi \mathbf{P}_{ex}(d,d)}} \cdot$$
$$\int_{-l_d}^{l_d} \exp\left(\frac{(x - \mu_{HI,ex,d})^2}{2\mathbf{P}_{ex}(d,d)}\right) dx \quad (21)$$

where $\mathbf{P}_{ex}$ is covariance matrix of ϵ_{ex} and $\mu_{HI,ex,d}$ can be written as:

$$\mu_{HI,ex,d} = \sum_{e=1}^{n} |\mathbf{S}_{ex}(d,e)|\mathbf{b}(e,d) + \sum_{e=1}^{n} |\mathbf{S}_{ex}(d,e)|\mathbf{f}_k(e,1) \quad (22)$$

For $P_{ND,ex,d}$, it can be written as:

$$P_{ND,ex,d} = \frac{1}{\sqrt{2\pi \mathbf{P}_{ex,k}(d,d)}} \cdot$$
$$\int_{-T_{\Delta_{ex,k,d}}}^{T_{\Delta_{ex,k,d}}} \exp\left(\frac{(y - \mu_{ND,ex,d})^2}{2\mathbf{P}_{ex,k}(d,d)}\right) dy \quad (23)$$

where $\mathbf{P}_{ex,k}$ is covariance matrix of $\Delta_{ex,k}$ and $\mu_{ND,ex,d}$ can be written as:

$$\mu_{ND,ex,d} = -\sum_{e=1}^{n} |\mathbf{S}_{ex}(d,e) - \mathbf{S}_{ex,k}(d,e)|\mathbf{b}(e,d)$$
$$+ \sum_{e=1}^{n} |\mathbf{S}_{ex}(d,e)|\mathbf{f}_k(e,1) \quad (24)$$

we can rewrite $P_{HI,ex,d} \cdot P_{ND,ex,d}$ as:

$$P_{HMI,5} = P_{HI,ex,d} \cdot P_{ND,ex,d}$$
$$= k_{ex,k} \int_{-T_{\Delta_{ex,k,d}}}^{T_{\Delta_{ex,k,d}}} \exp\left(\frac{(y - M + b_{ex,k})^2}{2\mathbf{P}_{ex,k}(d,d)}\right) dy -$$
$$k_{ex,k} k_{ex} \int_{-l_d}^{l_d} \int_{-T_{\Delta_{ex,k,d}}}^{T_{\Delta_{ex,k,d}}} \exp\left(-\frac{(y - M + b_{ex,k})^2}{2\mathbf{P}_{ex,k}(d,d)}\right)$$
$$\exp\left(-\frac{(x - M + b_{ex})^2}{2\mathbf{P}_{ex}(d,d)}\right) dx dy \quad (25)$$

where $k_{ex,k} = \frac{1}{\sqrt{2\pi \mathbf{P}_{ex,k}(d,d)}}$, $k_{ex} = \frac{1}{\sqrt{2\pi \mathbf{P}_{ex}(d,d)}}$, $y - M + b_{ex,k} = y - \mu_{ND,ex,d}$ and $x - M + b_{ex} = x - \mu_{HI,ex,d}$. The derivation of $P_{HMI,5}$ is similar to $P_{HMI,2}$, so the function image of $P_{HMI,5}$ is similar to Fig. 1. As for $b_{ex,k}$ and b_{ex}, the definition is same as b_i and b_0.

In order to evaluate navigation performance, we need to derive the equation of calculating VPL. When the integrity risk requirement I_{req} is specified, VPL can be derived from Eq. (15). Corresponding to Eq. (15), I_{req} is devided into five terms.

$$I_{req} \leq I_1 + I_2 + I_3 + I_4 + I_5 \quad (26)$$

Based on the first term in Eq. (15), the first term of Eq. (26) can be expressed as:

$$I_1 = \left[\bar{Q}\left(\frac{-VPL - b_{0,3}}{\sigma_{0,3}}\right) + Q\left(\frac{VPL - b_{0,3}}{\sigma_{0,3}}\right)\right] P_{H_0} \quad (27)$$

where function Q and $\bar{Q}$ are defined as:
$$Q(x) = \frac{1}{2\pi} \int_x^{\infty} \exp(-\frac{t^2}{2}) dt, \quad \bar{Q}(x) = 1 - Q(x) \quad (28)$$

In Eq. (15), the second term represents the system contains a specific fault H_i and the magnitude $\mathbf{f}_i$ of this fault model. I_2 in Eq.(26) is under this condition and it can be expressed as:

$$I_2 = \sum_{i=1}^{m} \max_{\mathbf{f}_i}\left(P(|\epsilon_0| > l|H_i, \mathbf{f}_i) \cdot P(|\Delta_i| < T_i|H_i, \mathbf{f}_i)\right) P_{H_i}$$
$$= \sum_{i=1}^{m} \left[\bar{Q}\left(\frac{-VPL - \mu_{HI,i,3}}{\mathbf{P}_0(3,3)}\right) + Q\left(\frac{VPL - \mu_{HI,i,3}}{\mathbf{P}_0(3,3)}\right)\right]$$
$$\cdot \left[Q\left(\frac{-T_{\Delta_{i,3}} - \mu_{ND,i,3}}{\mathbf{P}_i(3,3)}\right) - Q\left(\frac{T_{\Delta_{i,3}} - \mu_{ND,i,3}}{\mathbf{P}_i(3,3)}\right)\right] P_{H_i} \quad (29)$$

where $\mu_{HI,i,3}$, $\mathbf{P}_0(3,3)$ and $\mu_{ND,i,3}$, $\mathbf{P}_i(3,3)$ in Eq.(29) are bias and covariance corresponding to the maximum value of $P(|\epsilon_0| > l|H_i, \mathbf{f}_i) \cdot P(|\Delta_i| < T_i|H_i, \mathbf{f}_i)$.

As for the third and the fourth term of Eq. (26), these two terms represent the fault free model in exclusion function. The third term I_3 can be written as:

$$I_3 = \sum_{ex=0}^{m} \left[\bar{Q}\left(\frac{-VPL - b_{ex,3}}{\sigma_{ex,3}}\right) + Q\left(\frac{VPL - b_{ex,3}}{\sigma_{ex,3}}\right)\right] P_{H_0} \quad (30)$$

and the fourth term can be written as:

$$I_4 = \sum_{ex=0}^{m} \left[\bar{Q}\left(\frac{-VPL - b_{ex,3}}{\sigma_{ex,3}}\right) + Q\left(\frac{VPL - b_{ex,3}}{\sigma_{ex,3}}\right)\right] P_{H_{ex}} \quad (31)$$

The last term I_5 of Eq. (26) still exist the fault and its magnitude can affect the value of PHMI. This term can be calculated as:

$$I_5 = \sum_{ex=0}^{m} \sum_{\substack{k=1 \\ k \neq ex}}^{m_1} \max \mathbf{f}_k \Big(P(|\epsilon_{ex}| > l|H_k, \mathbf{f}_k) \cdot$$

$$P(|\Delta_{ex,k}| < T_{ex,k}|H_k, \mathbf{f}_k)) \Big) P_{H_k}$$

$$= \sum_{ex=0}^{m} \sum_{\substack{k=1 \\ k \neq ex}}^{m_1} \Big[\bar{Q} \left(\frac{-VPL - \mu_{HI,ex,3}}{\mathbf{P}_{ex}(3,3)} \right) +$$

$$Q \left(\frac{VPL - \mu_{HI,ex,3}}{\mathbf{P}_{ex}(3,3)} \right) \Big]$$

$$\cdot \Big[Q \left(\frac{-T_{\Delta_{ex,k,3}} - \mu_{ND,ex,3}}{\mathbf{P}_{ex,k}(3,3)} \right) -$$

$$Q \left(\frac{T_{\Delta_{ex,k,3}} - \mu_{ND,ex,3}}{\mathbf{P}_{ex,k}(3,3)} \right) \Big] P_{H_k}$$

$$(32)$$

where $\mu_{HI,ex,3}$, $\mathbf{P}_{ex}(3,3)$ and $\mu_{ND,ex,3}$, $\mathbf{P}_{ex,k}(3,3)$ in Eq. (32) are bias and covariance corresponding to the maximum value of $P(|\epsilon_{ex}| > l|H_k, \mathbf{f}_k) \cdot P(|\Delta_{ex,k}| < T_{ex,k}|H_k, \mathbf{f}_k)) P_{H_k}$.

From Eq. (27) to Eq. (32), the only variable is VPL. So we can derive the value of VPL by using the numerical method in APPENDIX E of [14]. In order to compute the maximum value in Eq. (29) and Eq. (32), we introduce a numerical method in the following section and it could seek the maximum value.

3.2 Numerical Method and Test Example

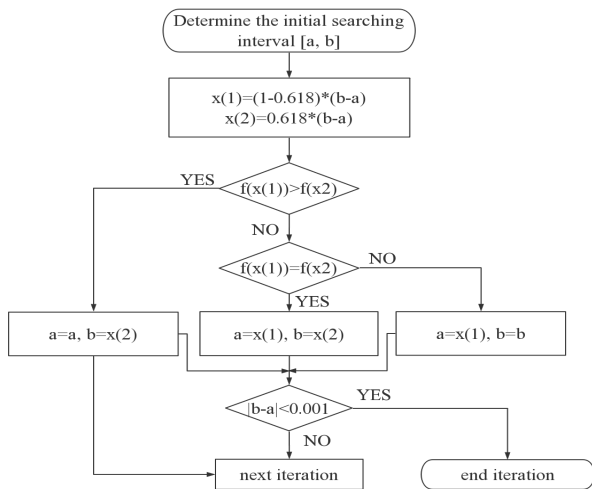To calculate the maximum value in Fig.3, we introduce a numerical method: optimization method.

Fig. 4 Flowchart of Optimization Method

Before we introduce the method in detail, we denote $f(x(k))$ as the maximum value of the function. At the beginning of optimization method, we first need to determine the interval where the extremum is located. Based on the properties of Probability Density Function (PDF) of Normal Distribution, the initial search interval is set to [0, T+37], where T is the threshold for test statistic. If we assume the extremum locates within [a, b]. The method chooses two point $x(1)$ and $x(2)$ in $[a, b]$ where $x(1) = (1 - 0.618) \times (b - a)$ and $x(2) = 0.618 \times (b-a)$. If $f(x(1)) > f(x(2))$, the search interval is changed to $[x(1), b]$. If $f(x(1)) < f(x(2))$, the search interval is changed to $[a, x(2)]$. Especially, when $f(x(1)) = f(x(2))$, the search interval is changed to $[x(1), x(2)]$. When $x(1)$ and $x(2)$ are close enough $(|x(1) - x(2)| < 0.01)$, the search will be terminated.

Take $Z = -(x - 5)^2 + 70$ as an example, the maximum value of Z is 70 and the corresponding point is 5. In order to find this maximum value, the initial interval is set to [4, 7]. Table 1 shows the result of optimization method with different termination conditions.

Table 1 Test Example Result

Termination Condition	Error($x(i) - x(k)$)	Time/s
1	-0.073	0.00042
0.6	-0.073	0.00060
0.2	0.0623	0.00099
0.1	0.0106	0.00210
0.05	-0.0410	0.00221
0.01	-0.0016	0.00284

4 ARIAM Test Platform

4.1 Hardware Description

Fig.5 shows the three important hardware parts of ARAIM test platform: GNSS antenna, GNSS receiver, users computer. When we operating ARAIM test platform, we first use chock ring antenna located on the top of SJTU GNC Lab (31.026105436N, 121.442347327E, 36.836202m) to receive GPS, BDS and GLONASS signals. Then, analog signals will be processed by multi-frequency GNSS receiver, which is able to convert the analog signals to digital signals and to provide users with the message of ephemeris and pseudorange. Next, digital signals will be transmitted to computer by serial communication. Fig. 6 and Fig. 7 shows the chock ring antenna and GNSS receiver (from ComNav, China) that we used to build ARAIM test platform.
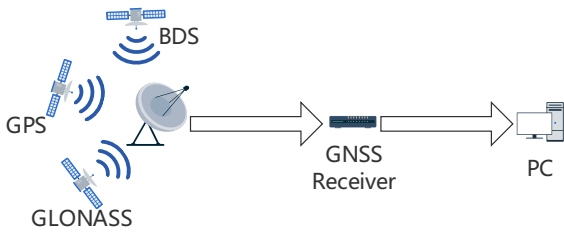
Fig. 5 Hardware of ARAIM Test Platform

Fig. 6 ComNav GNSS Receiver

Fig. 7 Chock Ring Antenna

4.2 Software Description

The software of ARAIM test platform consists of two parts: online version and offline version. For online version, when binary input stream is transmitted by serial communication from GNSS receiver to users computer, the computer first decode the binary input stream based on IEEE 754 protocol. After we acquiring the message of ephemeris and pseudorange from decoded binary input stream, local computer is able to calculate the users location and implement the ARIAM algorithm. Fig.8 shows the structure of online version ARAIM test platform. For offline version, it is designed for some harsh circumstance that local computer is malfunctioning and serial communication is interrupted. Due to GNSS receiver has 100 megabytes of memory, the lost data processed by GNSS receiver can be stored in the receiver as RENIX format. Then, by using RENIX file, we can calculate the users location and start running the ARAIM algorithm. Fig.9 shows the structure of offline version ARAIM test platform.
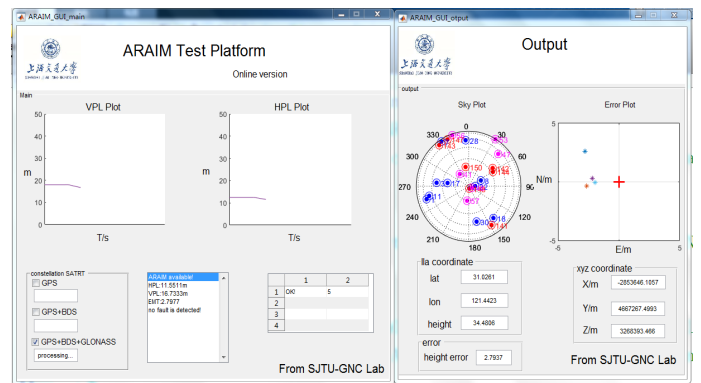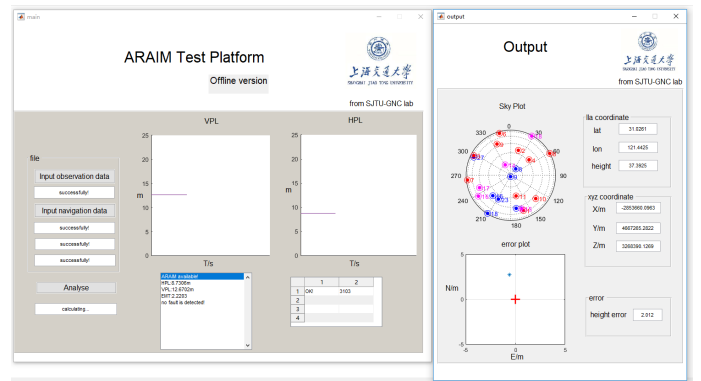

Fig. 8 Online ARAIM Test Platform

Fig. 9 Offline ARAIM Test Platform

5 Result

5.1 Global Almanac Data Result

We use 6-hour almanac data from International GNSS Service (IGS) to calculate the worldwide VPL and 99.5% coverage. For ARAIM Fault Detection (FD) algorithm and ARAIM Fault Detection and Exclusion (FDE) algorithm, based on the requirement of continuity [5], we analyse the VPL and 99.5% coverage. The

computational burden of ARAIM algorithm and our new method is also listed below.

Table 2 Computational Burden of Different Method

algorithm	method	Time(all)	Time(epoch)
FD	MHSS	3.28min	0.008s
	Tighter bound	12.87min	0.033s
FDE	MHSS	40.72min	0.104s
	Tighter bound	221min	0.568s

Table 3 VPL for ARAIM FD Algorithm

URA	bias	VPL(MHSS)	VPL(Tighter bound)
URA=0.5	b=0.1	15.75m	5.70m
	b=0.3	16.87m	6.60m
URA=1	b=0.1	20.59m	8.74m
	b=0.3	21.70m	9.67m
URA=1.6	b=0.1	27.87m	13.84m
	b=0.3	28.99m	15.25m

Table 4 Coverage for ARAIM FD Algorithm

URA	bias	coverage(MHSS)	coverage(Tighter bound)
URA=0.5	b=0.1	100%	100%
	b=0.3	100%	100%
URA=1	b=0.1	99.89%	100%
	b=0.3	99.89%	100%
URA=1.6	b=0.1	94.53%	99.14%
	b=0.3	94.02%	98.82%

Table 5 VPL for ARAIM FDE Algorithm

URA	bias	VPL(MHSS)	VPL(Tighter bound)
URA=0.5	b=0.1	33.01m	19.73m
	b=0.3	35.56m	23.79m
URA=1	b=0.1	43.92m	29.27m
	b=0.3	46.45m	32.93m
URA=1.6	b=0.1	60.38m	39.13m
	b=0.3	62.92m	40.76m

Table 6 Coverage for ARAIM FDE Algorithm

URA	bias	coverage(MHSS)	coverage(Tighter bound)
URA=0.5	b=0.1	81.59%	85.39%
	b=0.3	76.40%	79.12%
URA=1	b=0.1	51.93%	71.61%
	b=0.3	46.13%	60.76%
URA=1.6	b=0.1	8.35%	34.98%
	b=0.3	5.70%	23.21%

The results which are listed in Table 2, Table 3, Table 4, Table 5 and Table 6 show tighter bound ARIAM algorithm can lower the protection level and improve the coverage worldwid without increasing too much computational burden.

5.2 ARAIM Test Platform Result

Using ARAIM Test Platform, we collect 6-hour, three constellation (GPS, BDS, GLONASS) real-time data to verify the effect of our new method on navigation performance. The total time of processing 6-hour real time data using MHSS algorithm and tighter bound algorithm is 392 minute and 443 minute. For each epoch, the time of MHSS algorithm and tighter bound algorithm 1.09s and 1.23s respectively. Fig.10 shows the 6-hour positioning error. The average errors in east, north and up direction are 1.12m, 1.99m and 3.00m respectively.
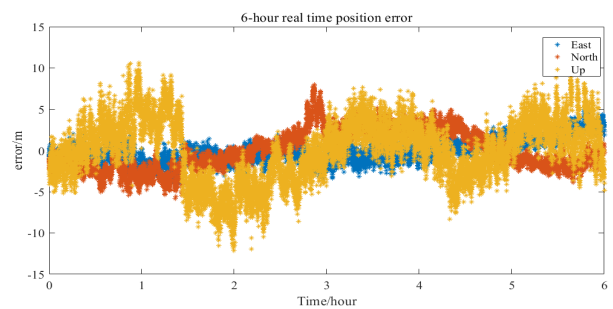
Fig. 10 6-hour Positioning Error

Fig.11 shows the 6-hour VPL by using ARAIM FD algorithm. The blue line, red line and yellow line in Fig.11 represent the VPL of single constellation, dual constellation and three constellation. Navigation performance increases with the number of constellations. Three constellation can provide the best navigation performance for user.
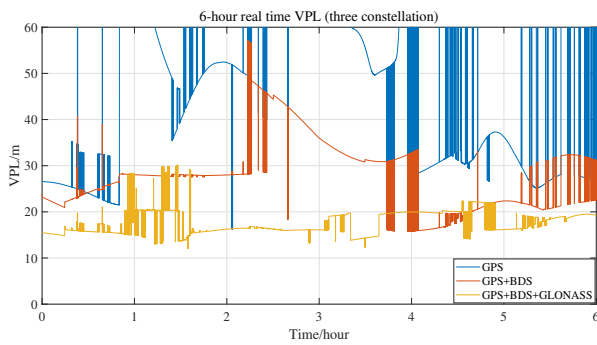
Fig. 11 VPL Using Different Constellations

Fig.12 shows the 6-hour VPL by using MHSS ARAIM FD algorithm and tighter bound ARAIM algorithm. When the test platform applies three constellations, VPL can be declined by our tighter bound ARAIM algorithm. the blue line and red line in Fig.12 represent the VPL of MHSS algorithm and tighter bound ARAIM algorithm.
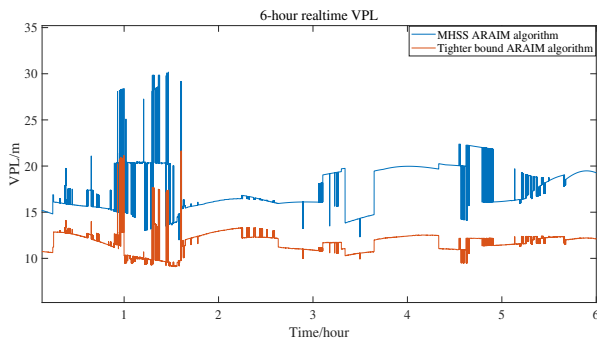

Fig. 12 VPL of Different Methods (URA=1, b=0.75)

6 Conclusion

In this paper, there are three main contributions. Firstly, we build ARIAM test platform which supports real-time integrity monitoring and post-processing integrity monitoring. Secondly, we find the bound of PHMI in ARAIM user algorithm is not tight enough and propose a new method to overcome this drawback. At lastwe use ARAIM Test Platform and the data form IGS to prove that our new method is able to improve the navigation performance without affecting real-time capability.

References

1. Mohamed, AH., and Schwarz, KP. Adaptive Kalman filtering for INS/GPS, *Journal of geodesy*, 73, 4, (1999), 193-203

2. Alexander, I. Perspective/navigation-the global positioning system, *IEEE spectrum*, 30, 12, IEEE, (1993), 36-38

3. Hofmann-Wellenhof, B,. Lichtenegger, H,. Wasle, E. GNSS–global navigation satellite systems: GPS, GLONASS, Galileo, and more, *Springer Science & Business Media*, (2007)

4. International Civil Aviation Organization (ICAO), Annex 10:Aeronautical Telecommunications. Volume 1: (Radio Navigation Aids), Amendment 84, published 20 July 2009, effective 19 November 2009, GNSS standards and recommended practices (SARPs) are contained in Section 3.7 and subsections, Appendix B, and Attachment D.

5. Zhai, Y. Ensuring navigation integrity and continuity using multi-constellation GNSS, PhD. Dissertation, Illinois Institute of Technology, Chicago, IL,(2018)

6. Parkinson, B., Axelrad, P. Autonomous GPS integrity monitoring using the pseudorange residual, *Navigation*, 35, 2, (1988), 255-274

7. Patrick, Y., Collins, R,. RAIM-FDE Revisited: A New Breakthrough In Availability Performance With nioRAIM (Novel Integrity-Optimized RAIM), *Proceedings of the 18th International Technical Meeting of the Satellite Division of the Institute of Navigation (ION GNSS)*, 53,1, (2006), 41-51

8. Ivanov, V., Gefan, G., and Gorbachev, O. Global empirical modelling of the total electron content of the ionosphere for satellite radio navigation systems, *Journal of Atmospheric and Solar-Terrestrial Physics*, 73,13, (2011), 1703-1707

9. El-Mowafy, A., and Yang, C. Limited sensitivity analysis of ARAIM availability for LPV-200 over Australia using real data, *Advances in Space Research*, 57, 2, (2016),659-670

10. Li, X., Zhang, X., and Ren, X., Fritsche, M., Wickert, J., and Schuh, H. Precise positioning with current multi-constellation global navigation satellite systems: GPS, GLONASS, Galileo and BeiDou, *Scientific reports*, 5 (2015), 8328

11. Aleshkin, AP., Myslivtsev, TO., Nikiforov, SV., Savochkin, PV., Sakhno, IV., Semenov, AA., and Troitskii, BV. Calculation of Navigation Corrections for a Single-Frequency GNSS Receiver Based on Satellite Radio Occultation Data, *Gyroscopy and Navigation*, 10 1, (2019), 15-20

12. Pan, W., Zhan, X., Zhang, X., and Liu, B. GNSS/INS Integrity Monitoring Considering Nominal Bias for Civil Aircraft CAT-I Approach, *AIAA Scitech 2019 Forum*, 0361, (2019)

13. Blanch, J., Walker, T., Enge, P., Lee, Y., Pervan, B., Rippl, Markus., Spletter, A., and Kropp, Victoria. Baseline advanced RAIM user algorithm and possible improvements, *IEEE Transactions on Aerospace and Electronic Systems*, 51 1, (2015), 713-732

14. Cassel, R. Real-Time ARAIM Using GPS, GLONASS, and Galileo, master thesis, Illinois Institute of Technology, (2017)

15. EU-U.S. Cooperation on Satellite Navigation Working Group C - ARAIM Technical Subgroup., Milestone 3 Report.Final Version., (2016)

16. Zhai, Y., Joerger, M., and Pervan, Boris. Continuity and availability in dual-frequency multi-constellation ARAIM, *Proceedings of the 28rd International Technical Meeting of the Satellite Division of the Institute of Navigation (ION GNSS)*, (2015)

17. Joerger, M., Chan, F., and Pervan, Boris. Solution Separation Versus Residual-Based RAIM, *NAVIGATION: Journal of the Institute of Navigation*, 61 4, (2014), 273-291